NAMT
94-007

The Simulation of Hysteresis in Nonlinear Systems

David Kinderlehrer
Ling Ma

Carnegie Mellon University

Research Report No. 94-NA-007

February 1994

Sponsors

U.S. Army Research Office
Research Triangle Park
NC 27709

National Science Foundation
1800 G Street, N.W.
Washington, DC 20550

To appear in Proc. SPIE Smart Structures and Materials 94,
Mathematics and Control in Smart Structures, Banks, H. T., ed.

The simulation of hysteresis in nonlinear systems

David Kinderlehrer and Ling Ma

Center for Nonlinear Analysis and Department of Mathematics
Carnegie Mellon University, Pittsburgh, PA 15213-3890

1. INTRODUCTION

Simulations of magnetic, magnetostrictive, and pseudoelastic behavior exhibit hysteresis. These systems have a highly nonlinear character involving both short range anisotropy and elastic fields and, when appropriate, dispersive demagnetization fields. In this report we discuss our experience with this type of computation and the applications which it may serve. Hysteresis occurs even in the absence of an imposed dynamical mechanism, for example a Landau-Lifschitz-Gilbert dissipation or a driving force and is symptomatic of the manner in which the system navigates a path through local minima of its energy space. It is robust in the sense that the shape of the loop is invariant over several decades of mesh refinement. It is not sensitive to the particular method. We implemented continuation based on the conjugate gradient method, although the same results were obtained by other methods as well. Nonetheless, the propensity of optimization procedures to become marooned at local extrema when applied to nonconvex situations presents a fundamental challenge to analysis. Understanding and controlling such phenomena present the opportunity to develop predictive tools and diagnostics.

We present some computational results and diagnostics, developed using methods of nonlinear analysis. As illustrations: Since the energy picture is mesh independent, computing on a fairly coarse grid suffices to establish its character. In a simple case described below, the width of the hysteresis loop may be determined analytically. For a magnetic system, this analysis rests on the introduction of a shadow energy for a simplifed version of the system. This simplified version suggests possible dispersive interactions which may be attributed to a shape-memory or pseudoelastic body. We provide a brief illustration of this.

A principal objective of this investigation is to study the magnetostrictive behavior of Terfenol-D,[1,5,6,7,12,13,14,15,16,17,18,21]. Complete details are given in [19]. Hysteresis in magnetic systems has been computed both by Preisach modeling [4,25,34,35] and by micromagnetics with various evolution mechanisms, eg. [10]. Recent related thoughts about hysteretic behavior, principally in shape memory or pseudoelastic materials, may be found in [2,3,11,20,26,27,28,30].

2. A MAGNETIC SYSTEM

2.1. Formulation

In the framework of micromagnetics, consider a two dimensional system governed by a magnetic anisotropy density subjected to an externally applied field. This gives rise to a stored energy to which we add the demagnetization energy, or the energy of the induced magnetic field. Employing the notations

m	magnetization	
$\varphi(m,x)$	anisotropy energy	(2.1)
H	applied magnetic field	
u	potential of demagnetization field,	

the energy of the system may be expressed, in appropriate units, in the form

$$E(H,m) = \int_\Omega (\varphi(m,x) - H\cdot m)\, dx + \frac{1}{2}\int_{\mathbb{R}^2} |\nabla u|^2 dx \tag{2.2}$$

$$\Delta u = \operatorname{div} m\chi_\Omega \text{ in } \mathbb{R}^2 \quad \text{and} \quad |m| = 1 \text{ in } \Omega.$$

Ω is the region occupied by the material. The second equation embodies Maxwell's Equations for magnetostatics. The constraint on m is the requirement that the material be magnetically saturated. In our computational study we choose $\Omega = (-L,L) \times (0,1)$, a rectangle. An equivalent form of the energy is

$$E(H,m) = \int_\Omega (\varphi(m,x) - H\cdot m)\, dx + \frac{1}{2}\int_\Omega \nabla u\cdot m\, dx \tag{2.3}$$

Linear magnetostriction may be accomodated in this framework without any significant change, cf. Clark [5]. A simple energy for a two dimensional linear magnetostrictive material is

$$\varphi(\varepsilon,m) = \varphi_{el}(\varepsilon) + \varphi_{el/mag}(\varepsilon,m) + \varphi_{an}(m), \tag{2.4}$$

$$\varepsilon = \frac{1}{2}(\nabla y + \nabla y^T),$$

where $y(x)$ denotes the deformation. The elastic energy $\varphi_{el}(\varepsilon)$ is a typical linear elastic energy. The elastic/magnetic interaction term has the form

$$\varphi_{el/mag}(\varepsilon,m) = \sum b_{ij}\varepsilon_{ij}m_i m_j .$$

Note that it is even in m. The anisotropy energy $\varphi_{an}(m)$ is the one which appears in (1.1). The analogue of (2.2) is

$$E(H,y,m) = \int_\Omega (\varphi(m,\varepsilon) - H\cdot m)\,dx + \frac{1}{2}\int_\Omega \nabla u\cdot m\,dx \tag{2.5}$$

Relaxation of funcionals having this form is discussed in [9]. Some forms for the anisotropy energy are, with $\kappa > 0$,

$$\varphi(m) = \kappa(m_2)^2 \qquad \text{uniaxial} \tag{2.6}$$

$$\varphi(m) = \kappa(m_1 m_2)^2 \text{ or } \frac{1}{2}\kappa(m_1^4 + m_2^4) \qquad \text{cubic} \tag{2.7}$$

$$\varphi(m) = \kappa(1 - q^{(1)}\cdot m)^2(1 - q^{(2)}\cdot m)^2, \quad |q^{(j)}| = 1 \tag{2.8}$$

In the uniaxial case (2.6), e_1 is the easy axis. This will be our primary concern here. For $(2.7)_1$, e_1 and e_2 are easy axes and for $(2.7)_2$, $e_1 \pm e_2$ are easy axes. For (2.8), the vectors $q^{(1)}$ and $q^{(2)}$ are easy axes. This form is useful when considering the projection onto a plane of a three dimensional situation. As suggested in (2.1), the anisotropy energy may vary with $x \in \Omega$. This will be the case when we model Terfenol, for example, or a thin film with a distribution of easy axes.

2.2 The computation of hysteresis

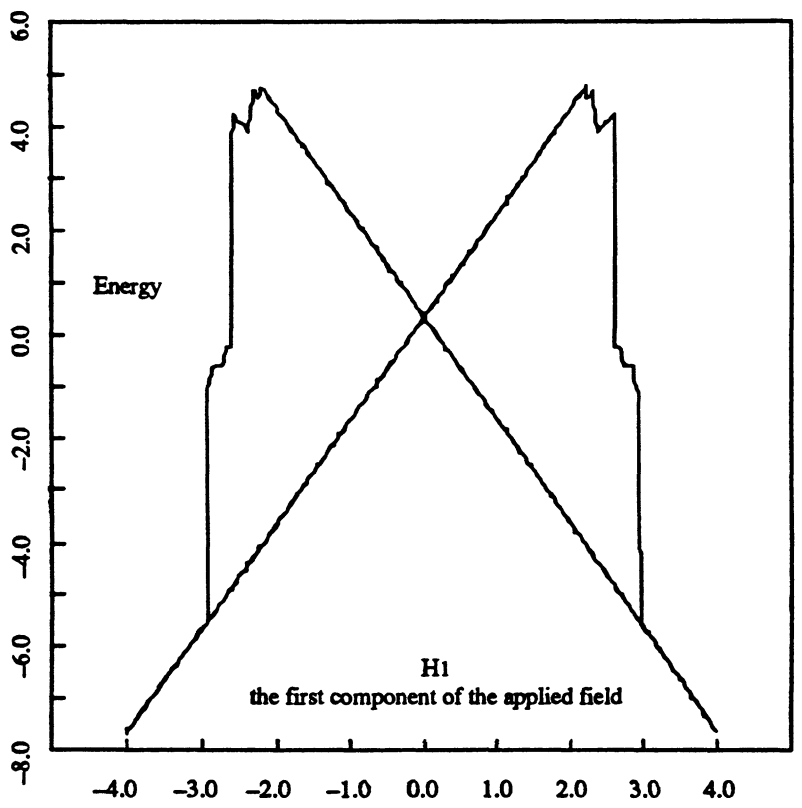

Figure 1. Computed hysteresis picture for uniaxial anisotropy energy (2.6) with $\kappa = 1.6$.

The hysteresis diagram for (2.2) is computed by continuation of solutions with respect to increasing and decreasing the applied magnetic field along the x_1-axis. The shown diagrams in Figures 1 and 2 are the overlaid graphs of $(H^k, E(H^k,m^k))$ and $(H^j, E(H^j,m^j))$ with the H^k an increasing sequence and the H^j a decreasing sequence of applied fields.

The computational domain is a rectangle $\Omega = (-L,L) \times (0,1)$, usually with $L = 1$, oriented so that the x_1 axis is an easy direction, and partitioned into $N_1 \times N_2$ squares of side length $h = 2L/N_1 = 1/N_2$ denoted by

$$\Omega_{ij} = \{x \in \Omega\colon ih - L < x_1 < (i+1)h - L,\ jh < x_2 < (j+1)h\},$$

$i = 0, \ldots, N_1 - 1$, $j = 0,1,\ldots,N_2 - 1$. The minimization of (2.2) is approximated in the space A_h by the Polak-Ribière version of the

conjugate gradient method [31,32] where

$$A_h = \{ m\colon m \text{ is constant on each } \Omega_{ij}, i = 0, \ldots, N_1 - 1,\ j = 0,1,\ldots,N_2 - 1\}.$$

The minimization algorithm requires the computation of energy and also the gradient of the energy with respect to the discrete variables for a given set of $m \in A_h$. We remark that the most expensive feature of these computations is the determination of the averages of ∇u on the cells Ω_{ij}, i.e.,

$$\overline{\nabla u}_{ij} = \frac{1}{h^2} \int_{\Omega_{ij}} \nabla u \, dx.$$

We refer to Luskin and Ma [22,23,24] for details. When computing elastic fields, the cells Ω_{ij} are further subdivided into triangles appropriate for finite element spaces.

The configuration begins at an absolute minimum of energy, or nearly so, for a large value of H_o and remains in this state until H^k changes sign. For these values of H^k, $m^k \approx m^0$, which we refer to as the precursor magnetization. This precursor magnetization is quite close to e_1.

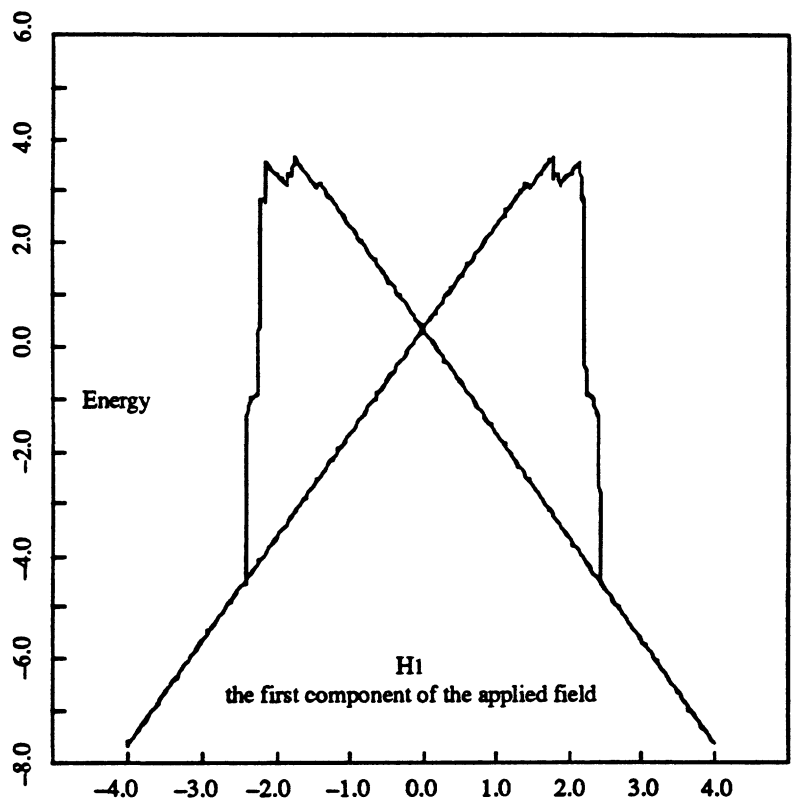

Figure 2. Computed hysteresis picture for cubic anisotropy $(2.7)_2$ with $\kappa = 1.6$.

The system then traverses a metastable regime where it does not realize minimum energy. Some small oscillations are observed in this regime. The metastable regime ends in a critical field range which appears to be characterized by the condition that the precursor magnetization becomes unstable at the critical field, H_{cr},

$$E(H_{cr},m) \le E(H_{cr},m^0) \quad \text{for appropriate } m. \tag{2.9}$$

In fact, it seems that the computation seeks to resolve the closure domains first. These are the boundary columns of the computational grid. We use this as the basis for our estimate of H_{cr}.

Near $H = H_{cr}$, the system suffers instability and witnesses rapid interior oscillations, the evolution of microstructural domain configurations, and finally resolution to a nearly uniform state of approximately absolute minimum energy. In this regime, the behavior of the system is analogous to the classical Stoner-Wohlfarth scenario [33]. Müller and Xu [28] also observe a stable/metastable/unstable/ stable sequence in the extension of shape memory ribbons. We do not see this behavior when

the applied field H is parallel to the hardest axis, which is x_2 in the uniaxial case and $x_1 \pm x_2$ in the cubic case. Indeed, there is almost no hysteresis in the hard axis uniaxial situation. Here we are discussing only the major loops of the system, which are the overlaid graphs mentioned above. We have also computed minor loops and the virgin magnetization curve.

2.3 Estimation of the critical field and the width of the hysteresis loop

A principal objective of this study is to illustrate that it is possible to predict the width of the hysteresis loop, at least in some situations. Here we describe such an estimate, which arises as a correction to the

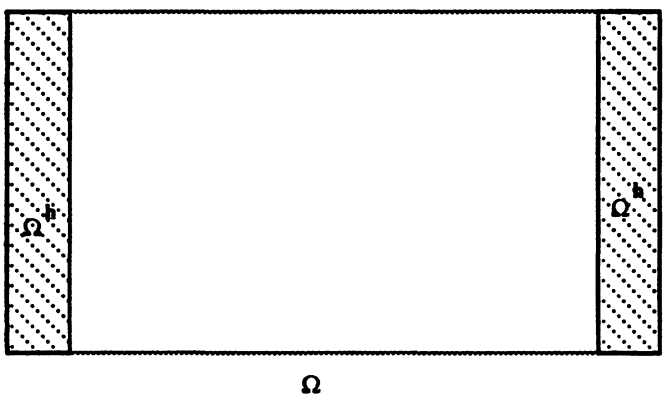

Figure 3. The computational region with the closure domain Ω^h.

classical Stoner Wohlfarth value, and compare it with the computational results. Analysis of the computational system is quite complicated owing to the $O(N^2)$ dependent variables. Instead we approximate it with a simpler system where the magnetization is assumed constant in each column. In this way we may profit from the observation that the closure domains are the first to switch; this can, in fact, be proved. With Ω^h the first and last columns of Ω, and Γ_1 and Γ_2 the right and left vertical boundaries of Ω, set

$$m = m^{(h)} = \begin{cases} \xi & \text{in } \Omega^h \\ e_1 & \text{in } \Omega\backslash\Omega^h \end{cases}, \quad |\xi| = 1, \text{ and} \tag{2.10}$$

$$\psi^{(h)}(H,\xi) = \frac{1}{|\Omega^h|}\left(E(H,m^{(h)}) - E(H,e_1)\right) \quad \text{and} \quad \psi^{(o)}(H,\xi) = \lim_{h\to 0} \psi^{(h)}(H,\xi). \tag{2.11}$$

Our simpler system, which we refer to as a *shadow system*, has the energy

$$E_s(H,\xi) = E(H,e_1) + |\Omega^h|\,\psi^{(o)}(H,\xi). \tag{2.12}$$

This expression may be explicitly computed and the result is

$$\psi^{(o)}(H,\xi) = \varphi(\xi) - \varphi(e_1) + (\xi_1 - 1)(\lambda - H_1) + \tfrac{1}{2}(\xi_1 - 1)^2, \tag{2.13}$$

$$\lambda = \lim_{h\to 0} \fint_{\Omega^h} \frac{\partial w}{\partial x_1}\,dx = \int_{\Gamma_1} \frac{\partial w}{\partial x_1}\,dx_2 = \frac{1}{2} + \frac{1}{2\pi}\int_0^1 \theta_2(z)\,dx_2, \text{ where} \tag{2.14}$$

$$\Delta w = \frac{\partial}{\partial x_1}\chi_\Omega \quad \text{in } \mathbb{R}^2. \tag{2.15}$$

The modern theory of differential equations and the classical theory of singular integrals, cf. Muskhelishvili [29], may be employed to tell us that

$$\frac{\partial w}{\partial z}(z) = \frac{1}{2\pi i}\int_{\Gamma_1}\frac{1}{t-z}dt + \frac{1}{2\pi i}\int_{\Gamma_2}\frac{1}{t-z}dt \quad , z \in \mathbb{R}^2\backslash\Gamma_1\cup\Gamma_2. \tag{2.16}$$

In particular, with $\theta_j(z)$ is the angle subtended by z and the segment Γ_j,

$$\frac{\partial w}{\partial x_1}(z) = \frac{1}{2\pi}(\theta_1(z) + \theta_2(z)), \; z \in \mathbb{R}^2\backslash\Gamma_1\cup\Gamma_2. \tag{2.17}$$

For $\varphi(\xi)$ given by (2.6) or $(2.7)_1$, uniaxial or cubic with x_1 - axis easy, $m = e_1$ is a local minimum of (2.12) when $H_1 > -H_{cr}$ for

$$H_{cr} = 2\kappa - \lambda. \tag{2.18}$$

For these φ, the classical Stoner-Wohlfarth value of the critical field is $H_{SW} = 2\kappa$. The width of the hysteresis loop is $2H_{cr} = 4\kappa - 2\lambda$.

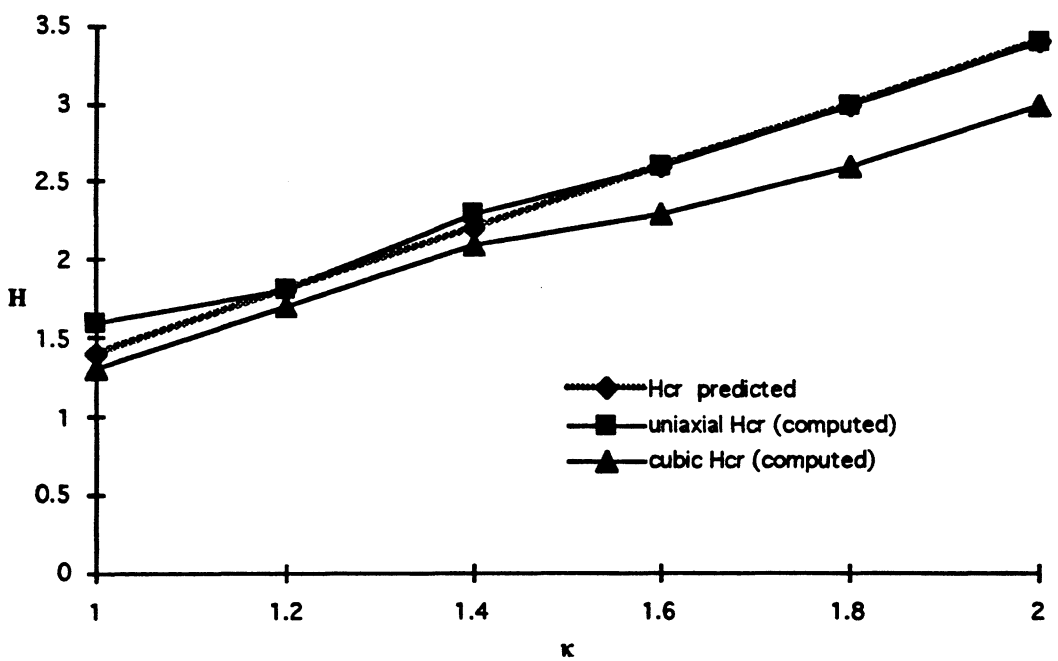

Figure 4. Comparison of predicted and computed critical field

2.4. Comparison with computation

The graph above summarizes our computational results. The data for both cases were taken from

computations on a 16×8 grid but these were identical to the results from a 32×16 grid. In the uniaxial case the predicted value is nearly identical to the computed one. Samples of graphical renderings of the computations appear in

Figures 1 and 2. The range of values of the anisotropy constant κ was chosen so the energy stored in a body of constant magnetization was comparable to the induced field energy. We suspect that the variation we see in the cubic case owes primarily to the inadequacy of $m_0 = e_1$ to serve as a precursor magnetization. A better precursor magnetization in this case might be somewhat tilted from the x_1 - axis at the four corners of Ω, which would require a more careful shadow energy.

2.5. Shadow energy

We now introduce a more complete shadow energy. Divide $\Omega = (0,2L) \times (0,1)$ into N columns D_j separated by vertical segments T_j,

$$T_j = \{ \operatorname{Re} z = a_j \}, \quad a_j = jh, \text{ with } D_j = \{ a_{j-1} < \operatorname{Re} z < a_j \} \cap \Omega, \quad j = 0,1,\ldots,N.$$

Consider magnetizations and induced field potentials

$$m = \sum_1^N \xi^j \chi_{D_j}, \quad \xi^j = \xi^{N-j}, \quad |\xi^j| = 1 \quad \text{and} \quad u \in H^1_{loc}(\mathbb{R}^2): \ \Delta u = \operatorname{div} m. \tag{2.19}$$

The exact induced field energy is given by

$$\frac{1}{2} \int_\Omega \nabla u \cdot m \, dx = \frac{1}{2} \sum \int_{D_j} \nabla u \cdot \xi^j \, dx . \tag{2.20}$$

This may be approximated by assuming that

$$\int_{D_j} \nabla u \cdot \xi^j \, dx \approx h \int_{T_j} \nabla u \cdot \xi^j \, dx_2,$$

which leads to the determination of a symmetric matrix (a_{jk}) of non-negative terms, $a_{kk} = 0$, such that

$$\frac{1}{2} \int_\Omega \nabla u \cdot m \, dx \approx \frac{1}{2} h \sum (\xi^j_1)^2 + \frac{1}{2} h \sum_{j \neq k} a_{jk} (\xi^j_2 \xi^k_2 - \xi^j_1 \xi^k_1) \tag{2.21}$$

Let $\varphi^k(m)$ denote the anisotropy energy in the column D_k. We then obtain an approximate or shadow energy for our computational system of the form

$$E_s(H,m) = h \sum \left(\varphi^j(\xi^j) + \frac{1}{2}(\xi^j_1)^2 - H\xi^j_1 \right) + \frac{1}{2} h \sum_{j \neq k} a_{jk} (\xi^j_2 \xi^k_2 - \xi^j_1 \xi^k_1). \tag{2.22}$$

This expression can be used to predict the behavior of the computation when e_1 is a hard axis as well as to recover the estimate (2.19). There is also a Young Measure limit version which has potential in the study of randomly distributed easy axes.

3. SHAPE MEMORY OR PSEUDOELASTIC SYSTEMS

Our conception is that most nonconvex computational optimization problems result in hysteretic behavior. As an example we have begun investigation of the Ericksen bar [8], which is a one dimensional version of a shape memory or pseudoelastic material. Hysteretic patterns of stress vs. load parameter in the extension of shape memory ribbons have been reported by Müller and Xu [28], as cited earlier, and by Ortin [30]. Their observations, while quite different, share certain features, in particular the sequence of states passing from stable to metastable to unstable. These experiments, in which the orientation of the sample was not recorded, suggest attempting a simulation in one space dimension with an energy density which is not convex. This amounts to studying the well known Ericksen bar. The computation becomes a one dimensional version of (2.1), without, however, the induced field energy. We reproduced the general features of the experiments, but further investigation is necessary to understand if many details are also reproduced by our computations. For the example illustrated in Figure 5, we computed

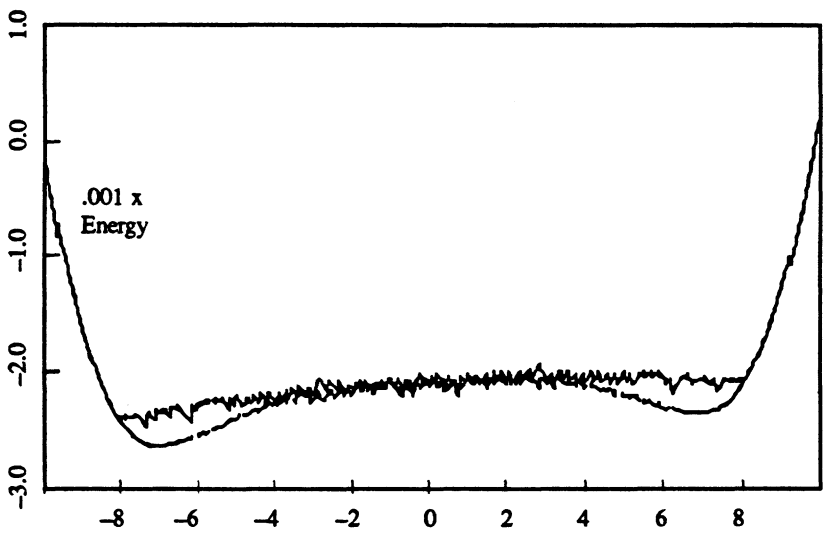

Figure 5. Computed hysteresis diagram for an Ericksen bar

$$E(\tau) = \int_0^1 \varphi(u')\,dx \quad \text{subject to } u(0) = 1 \text{ and } u(1) = \tau, \tag{3.1}$$

$$\varphi(t) = t^2(t^2 - 100) + 20t. \tag{3.2}$$

by continuation with respect to the loading parameter τ. Note that $\varphi(0) = 0$ suggesting that the computed configuration is rather close to the Maxwell line.

The shadow energy for the magnetic system suggests a possible surface energy correction to (3.1) which may bring the Müller and Xu theory into sharper focus. Writing ε for strain, a more general energy, written in discretized form, is

$$E(\varepsilon,\tau) = h\sum\left(\varphi(\varepsilon^j) + \tfrac{1}{2}a(\varepsilon^j)^2\right) - \tfrac{1}{2}h\sum_{j\neq k} a_{jk}\,\varepsilon^j\varepsilon^k \tag{3.3}$$

In the simplest case, consider only nearest neighbor interactions of equal strength so that

$$\sum_{j\neq k} a_{jk}\,\varepsilon^j\varepsilon^k = b\sum \varepsilon^j\varepsilon^{j-1}\ .$$

Assuming that the $\{\varepsilon^j\}$ are nearly in the energy wells α_1 and α_2 of φ, $a = b$, and that

$$\text{Prob}\{\varepsilon^j \approx \alpha_1\} = p \quad \text{and} \quad \text{Prob}\{\varepsilon^j \approx \alpha_2\} = 1 - p,$$

one finds that, in agreement with [28],

$$\text{Exp}\left\{\tfrac{1}{2}a_o(\varepsilon^j)^2 - \tfrac{1}{2}a_o\sum \varepsilon^j\varepsilon^{j-1}\right\} = a_o(\alpha_1 - \alpha_2)\,p(1-p). \tag{3.4}$$

Finally, assuming that $a = O(\frac{1}{h}) = \frac{a_o}{h} + a_1 + \ldots$, it is easy to compute that in the limit at $h \to 0$, we obtain the functional

$$E(u) = \int_0^1 \left(\varphi(u') + \tfrac{1}{2}a_o(u'')^2\right)dx\ . \tag{3.5}$$

This gives rise to a one dimensional Ginzburg-Landau Equation.

4. ACKNOWLEDGMENTS

This research was supported in part by the Air Force Office of Scientific Research, the Army Research Office, and the National Science Foundation. Computational facilities were made available by the National Science Foundation through a grant to the Pittsburgh Supercomputer Center.

5. REFERENCES

[1] Al-Jiboory, M. and D. G. Lord, Bi, Y.J., Abell, J. S., and Hwang, A. M. H., and Teter, J. P. Magnetic domains an microstructural defects in Terfenol-D, J. Appl. Phys. (to appear)

[2] Ball, J. M.,Chu, C., and James, R. D. Metastability and hysteresis in elastic crystals (to appear)

[3] Bruno, O. Quasi-static dynamics and pseudoelasticity in polycrystalline shape-memory wires, *Mathematics in Smart Structures, Smart Structures and Materials '94*, Proc. SPIE vol. 2192 (Banks, H. T., ed)

[4] Charap, S. and Ktena, A. Vector Preisach modeling, J. Appl. Phys.

[5] Clark, A. E. 1980 Magnetostrictive rare earth - Fe_2 compounds, *Ferromagnetic Materials, Vol 1* (Wohlfarth, E. P. ed) North Holland, 532 - 589

[6] De Simone, A. 1993 Energy minimizers for large ferromagnetic bodies, Arch. Rat. Mech. Anal., 125, 99-144

[7] De Simone, A. 1994 Macroscopic response of magnetostrictive materials to applied magnetic fields, *Mathematics in Smart Structures, Smart Structures and Materials '94*, Proc. SPIE vol. 2192 (Banks, H. T., ed)

[8] Ericksen, J. 1975 Equilibrium of bars, J. Elasticity, 5, 191-201

[9] Fonseca, I., Kinderlehrer, D., and Pedregal, P. Energy functionals depending on elastic strain and chemical composition, Calc. Var. Diff Eqns (to appear)
[10] Giles, R., Alexopoulos, P. S., and Manuripur, M. 1992 Micromagnetics of thin film cobalt-based media for magnetic recording, Comp. in Physics, 6, 53-70
[11] James, R. D. 1994 Metastability in phase transformations,*Mathematics in Smart Structures, Smart Structures and Materials '94*, Proc. SPIE vol. 2192 (Banks, H. T., ed)
[12] James, R. D. and Kinderlehrer, D. 1990 An example of frustration in a ferromagnetic material, Nematics: Mathematical and Physical Aspects, (Coron, J.-M., Ghidaglia, J.-M., and Hélein, F., eds), Kluwer NATO ASI series, 201-222
[13] James, R. D. and Kinderlehrer, D. 1990 Frustration in ferromagnetic materials, Cont. Mech. Therm., 2, 215-239
[14] James, R. D. and Kinderlehrer, D. 1992 Frustration and microstructure: an example in magnetostriction, *Prog Part Diff Eqns: calculus of variations, applications* (Bandle, C. et. al., eds) Pitman Res Notes Math 267, 59-81
[15] James, R. D. and Kinderlehrer, D. 1993 A theory of magnetostriction with application to $TbDyFe_2$ Phil. Mag. B, 68.2, 237-274
[16] James, R. D. and Kinderlehrer, D. 1993 Mathematical approaches to the study of smart materials, *Mathematics in Smart Structures, Smart Structures and Materials '93*, Proceedings SPIE vol. 1919, (Banks, H. T., ed.) 2-18
[17] James, R. D. and Kinderlehrer, D. 1993 Twinned structures in terfenol, Proc. ICOMAT
[18] Keane, M. K. and Rogers, R. C. A finite dimensional model problem in ferromagnetism, J. Int. Mat. and Struct. (to appear)
[19] Kinderlehrer, D., and Ma, L. to appear
[20] Leo, P., Shield, T., and Bruno, O. 1993 Transient heat transfer effects on the pseudoelastic behavior of shape-memory wires, Acta metall. mater. 41, 2477-2485
[21] Lord, D., Elliot, V., Clark, A. E., Savage, H. T., Teter, J. P., and McMasters, O. D. 1988 Optical observation of closure domains in Terfenol-D single crystals, IEEE Trans. Mag. 24, 1716-1718
[22] Luskin, M. and Ma, L. 1992 Analysis of the finite element approximation of microstructure in micromagnetics, SIAM J. Num Anal., 29, 320-331
[23] Luskin, M. and Ma, L. 1993 Numerical optimization of the micromagnetics energy, *Mathematics in Smart Structures, Smart Structures and Materials '93*, Proceedings SPIE vol. 1919, (Banks, H. T., ed.) 19-29
[24] Ma, L. 1993 Computation of magnetostrictive materials, *Mathematics in Smart Structures, Smart Structures and Materials '93*, Proceedings SPIE vol. 1919, (Banks, H. T., ed.) 47-54
[25] Mayergoyz, I. D. 1991 *The Preisach Model for Hysteresis*, Springer
[26] Müller, I. 1989 On the size of the hysteresis in pseucoelasticity, Cont. Mech. Therm., 1, 125-142
[27] Müller, I. and Huo, Y. 1993 Nonequilibrium thermodynamics of pseudoelasticity, Cont. Mech. Therm., 5, 163-204
[28] Müller, I. and Xu, H. 1991 On the pseudoelastic hysteresis, Acta Metall., 39, 263-271
[29] Muskhelishvili, N. I. 1992 *Singular Integral Equations*, Dover (reprint of 1953 Noordhoff edition)
[30] Ortin, J. 1992 Preisach modeling of hysteresis for a pseudoelastic Cu-Zn-Al single crystal, J. Appl. Phys ,71,1454-1461
[31] Polak, E. 1971 *Computational methods in optimization* , Academic Press
[32] Stoer, J. and Bulisch, R. 1993 *Introduction to numerical analysis, 2nd edition*, Springer
[33] Stoner, E. C. and Wohlfarth, E. P. 1948 A mechanisim of magnetic hysteresis in heterogeneous alloys, Phil. Trans. Royal Soc. (London) Sect A, 240, 599-642
[34] Visintin, A. *Differential models of hysteresis*, Springer
[35] Wiesen, K. and Charap, S. 1987 Vector Preisach modeling, J. Appl. Phys., 61, 4109-4021